Talanta 134 (2015) 530–537

Contents lists available at ScienceDirect

Talanta

journal homepage: www.elsevier.com/locate/talanta

Evaluation and modelling of dissolved organic matter reactivity toward As^{III} and As^{V} – Implication in environmental arsenic speciation

V. Lenoble [a,*], D.H. Dang [a,*], M. Loustau Cazalet [a], S. Mounier [a], H.-R. Pfeifer [b], C. Garnier [a]

[a] Laboratoire PROTEE, Université du Sud Toulon Var, BP 20132, 83957 La Garde Cedex, France
[b] IMG-Centre d'Analyse Minerale, Universite de Lausanne, Faculté de Géosciences et Environnement, Bâtiment Anthropole, CH-1015 Lausanne, Switzerland

ARTICLE INFO

Article history:
Received 2 August 2014
Received in revised form
18 November 2014
Accepted 22 November 2014
Available online 9 December 2014

Keywords:
Arsenic
SRHA
Cationic bridge
Dialysis
Fluorescence
Modelling

ABSTRACT

Many studies have been carried out to identify dissolved organic matter–trace metals interactions, as organic matter (OM) was demonstrated to be a governing parameter of metals speciation. Concerning arsenic (As), such OM–As studies are scarce and concluded that, when As binding occurred, it was probably through cationic bridges or, in some cases, directly. Yet, analytical proofs remained complex to obtain. In this work, As binding with Suwanee River Humic Acid (SRHA), as an example of dissolved organic matter, was studied, considering both As^{III} and As^{V}, at various pH and in absence/presence of Na and Ca. Dialysis, fluorescence measurements and PHREEQC modelling were performed to identify and characterize the mechanisms at work for the various performed experiments. It was observed that As^{III} binding on SRHA occurred through direct SRHA–As^{III} binding and that neither Na nor Ca presence modify this mechanism. As^{V} appeared to be also bound by SRHA through direct interaction, but suffered from the competition of Na for the SRHA binding sites. Oppositely, in presence of Ca, the overall As^{V}–SRHA binding was significantly enhanced, Ca acting as an efficient cationic bridge through the formation of an SRHA–Ca–As^{V} ternary complex. All the obtained data were satisfactorily simulated using a unique set of binding parameters which can therefore be implemented in any speciation code to better address As behaviour in environmental conditions.

1. Introduction

People are more and more concerned about the contamination of their environment, but their notion of toxicity remains linked to the total concentration of undesirable elements. However, to correctly predict a potential toxic effect, it is necessary to determine the various species of an element in the considered environment. Such distribution will change according to the ecosystem physical–chemical parameters and the present co-ions. Concerning arsenic (As), its distribution within a sample can be partly determined by the existing analytical techniques, which can provide information on arsenic total concentration, its main inorganic species in aquatic environments (As^{III} and As^{V}), and some organic forms. Hyphenated methods can provide a more precise distribution by also considering the methylated and arsenosugars forms, e.g. HPLC–ICP-MS [1,2], HPLC–HG-AAS [3], HPLC–HG-AFS [4], HG-AAS [5,6] or even liquid–liquid micro extraction-ET-AAS [7,8]. Yet, there is a lack of analytical techniques to directly measure the arsenic linked to the organic matter of a sample, as such fraction is usually reached through separation prior to analysis, for example by dialysis [9,10].

In the case of metals, it is now widely accepted that their distribution and behaviour are governed by organic matter (OM) [11,12]. Deriving from degradation, recombination of small molecules, exudates or bacterial production, OM is a very complex mixture of molecules, whose properties depend on its origin and age [13]. Various techniques are used to characterize OM, considering it as a bulk e.g. TOC, DOC [14,15], SUVA [16], or pointing out specific properties, e.g. using fluorescence [14,17–19], FTIR [20] or NMR [21]. OM influence on metal mainly occurs through complexation by specific sites [22,23], defined by their concentration, acidity and complexation constants. From the various usable approaches, such interactions are often brought out by fluorescence quenching [24,25]. According to Ryan and Weber [26], fluorescence quenching takes place when the complexation of a species occurs near a fluorescent site, leading to a modification of the fluorescence intensity. In the literature, studies dealing with the interactions between arsenic and organic molecules such as proteins through fluorescence quenching can be found [27] in order to develop new field analytical techniques. Yet, to the best of our knowledge, fluorescence quenching has never been used to specifically identify and characterize the interactions between arsenic and organic matter. Such is the purpose of this work.

The determination of As distribution either through its inorganic but also its organic species is of importance as this element poses a human health risk to millions of people worldwide [28,29].

* Corresponding authors. Tel.: +33 494142355; fax: +33 494142168.
E-mail addresses: lenoble@univ-tln.fr (V. Lenoble), dang@univ-tln.fr (D.H. Dang).

http://dx.doi.org/10.1016/j.talanta.2014.11.053
0039-9140/

Arsenic behaviour has largely been studied either under laboratory conditions [30–33] or directly on site [34–36] leading to a global comprehension of its interactions with inorganic fraction but seldom with the organic one. In the literature, when As and organic matter are considered at the same time, it is usually to define the influence of OM on As adsorption/desorption or oxidation. It is now more and more of concern to understand the real role of organic matter itself upon As. For example, organic matter was clearly shown to play a role in As dynamics in sediments or porewater (and thus potentially in other natural samples), even in the presence of inorganic phases [4]. It has been shown that OM can mobilise As from soil or sediment Fe oxides [37–40] or reduce As adsorption on Fe or Al oxides [40]. Few studies focused on determining direct organic matter–As interactions. The results showed that As (as As^{III} or As^{V}) binding occurred either through cationic bridges [10,41–45] or directly, through OM functional groups [9]. Such contrasted results can be explained by the important variability of organic matter, which hardens such kind of study. Another reason is the lack of analytical tool to specifically determine organic-retained As species, as explained before.

This complexity, added to the analytical locks, led to the fact that such organic–As fraction is often not taken into account within geochemical studies. According to As chemistry, inorganic fraction is probably governing this element distribution in an ecosystem. Yet, under extreme conditions such as anoxia, As distribution can change. To reach a global understanding of As behaviour in such kind of environment (e.g. rice paddy fields, deep sediment, acid mine drainage, etc.), speciation codes are often used. However, the most used speciation codes (PHREEQC, MINEQL, etc.) are currently lacking data concerning the interactions between OM and As^{III}, which are respectively the most reactive ligand and the main As species within these conditions.

The aims of this work were (1) to propose analytical tools able to specifically study arsenic organic fractions, (2) to identify the interactions between organic matter and As (either as As^{III} and As^{V}) and (3) after modelling, to implement the current speciation codes with appropriate binding parameters. The chosen organic matter was Suwannee River Humic Acid (SRHA), as it is well defined and often use as a model for organic matter (e.g. [23]). In order to identify and give an analytical evidence of SRHA–As interactions, dialysis, voltammetry and fluorescence quenching were associated. Such tools are often used to characterize OM and metals interactions (e.g. [24,46]). Yet, as As chemistry significantly differs to that of trace metals, this tools combination needs peculiar experimental setups. Furthermore, by the simultaneous modelling of fluorescence and voltammetry results by an unique set of parameters, and by PHREEQC modelling, SRHA–As^{III}, SRHA–As^{V} as well as ternary complex SRHA–As^{V}–Ca interaction constants were determined. Such results could improve the way As distribution in the environment is usually defined and modelled.

2. Experimental

2.1. Materials

All solutions were prepared with mQ water (18.2 MΩ, Millipore). All glassware was cleaned by soaking in 10% HNO_3 and rinsed with mQ water.

The arsenite stock solution was prepared from 1000 $mg_{As(III)}\,L^{-1}$ stable solution (Aldrich, purity > 99%). The arsenate stock solution was prepared by dissolving the appropriate amount of $AsHNa_2O_4 \cdot 7H_2O$ (Fluka, purity > 99%) in mQ water. The Cu^{II} solution was a 1000 $mg\,L^{-1}$ standard solution (Aldrich, purity > 99%) used without dilution. The Se^{IV} solution was prepared daily from the 1000 $mg\,L^{-1}$ standard solution (Aldrich, purity > 99%). 0.5 M Ca and 1 M Na solutions were respectively prepared from $CaCl_2$ (Merck, Pro Analysis) and NaCl (Fisher, Pro Analysis). All other chemicals were of analytical grade and used without further purification.

Suwannee River Humic Acid (SRHA) was purchased from the International Humic Substance Society (IHSS) and dissolved in mQ water in order to prepare a 15 $mg_C\,L^{-1}$ stock solution.

2.2. Analytical tools

Total As determinations were performed by Graphite Furnace Atomic Absorption Spectrometry (GFAAS) on a Thermo GF95Z instrument with Zeeman background correction. All measurements were based on integrated absorbance and carried out using a hollow-cathod lamp (Thermo) at 193.7 nm. All analytical parameters are detailed in a previous work [47]. The linearity range was 0.05–1 μM, the accuracy and RSD were 5% and ± 7%, respectively.

As^{III} measurements were performed by voltammetric measurements on a Metrohm-EcoChemie stand controlled by the GPES 4.9 software [48]. This apparatus is composed of a potentiostat/galvanostat (μAutolab I) connected to the measurement stand (VA663), comprising a static mercury drop electrode (SMDE), a reference (Ag/AgCl/KCl 3 M) and an auxiliary glassy carbon electrode. Arsenic was measured as As^{III} through the formation of an intermetallic compound with Cu and Se ($Cu_xSe_yAs_z$). All analytical measurement parameters are detailed in the aforementioned publication [49].

Dissolved organic carbon (DOC) in solution was measured with a Shimadzu TOC-V_{CSH} analyser, calibrated using sodium hydrogenophtalate standard solutions. The limit of detection is 0.1 $mg_C\,L^{-1}$ and the linearity ranged from 0.1 to 50 $mg_C\,L^{-1}$.

Major ions were analysed by ionic chromatography (Dionex, DX-120): SO_4^{2-}, Na^+, K^+, Mg^{2+}, Ca^{2+}. Anionic and cationic columns were loaded with quaternary ammonium (AS9-HC) or carboxylate-functionalized (CS12-A) groups, respectively. Anionic and cationic eluents were 9 mM Na_2CO_3 (Prolabo, Pro Analysis) and 20 mM CH_4SO_3 (Acros, Pro Analysis), respectively. In both cases the flow rate was 1 $mL\,min^{-1}$, and separated ions were quantified by conductimetry. Quality Control for ionic chromatography and organic carbon measurements was checked by the determination of elements concentration in "River Water Reference Material" (MISSIPPI-03, Environment Canada), which are in good agreement with the certified data (data not shown).

The interactions between SRHA and As were studied in 1-cm quartz cuve by UV–vis fluorescence spectroscopy on a HITACHI Fluorescence Spectrophotometer F 4500. The excitation and emission ranges were 250–500 and 250–600 nm, respectively, measured every 5 nm. Fluorescent properties led to the characterisation of molecules or OM through the measurement of excitation-emission fluorescence matrices (EEM) [50,51]. An algorithm based on PARAFAC statistical methods [52,53] was used to decompose all the measured EEMs (51 in total), previously corrected from inner-effect [54], in a set of common and identical fluorescent components. This decomposition provides a precise monitoring of the modifications of OM properties due to the variation of the contribution of each fluorescent component. More information on fluorescence decomposition is presented elsewhere [55]. In this study, each fluorescence spectrum was successfully reconstructed by a linear combination of 2 components with 98.5% of recovery. The variation of these two components as a function of increasing As^{III} and As^{V} concentrations and the presence of co-existing cations (Na and Ca) was considered. Due to a technical problem, the fluorescence results of SRHA–As^{III} experiment without cation addition were not exploitable. Such measurements and signal decomposition grant information on the interactions between SRHA and trace elements by the study of fluorescence quenching [24,56–58] The results will be discussed in parallel to the modelling results.

2.3. Experiments

For each set of experiments, SRHA (15 $mg_C\,L^{-1}$) and As were mixed inside a dialysis bag (Spectrum membrane, 500 Da), which was allowed to soak for 96 h in an As-free counter-dialysate solution at the same pH (buffer in both solutions) and ionic strength than the retentate. This contact time was validated for As^{III} and As^{V} experiments (data not shown), and was in good agreement with the literature [10]. Arsenic not retained by SRHA inside the dialysis bag will cross the membrane to reach the diffusate, whereas, if binding occurs, SRHA–bound As will remain inside the dialysis bag. Arsenic in the diffusate was labelled hereafter in the text as "free As". Arsenic considered as retained on SRHA (hereafter labelled in the text as "SRHA–bound As") corresponds to the calculated difference between the known As amount placed inside the dialysis bag (labelled as "total As concentration") and the free As which crossed the membrane. Experiments were performed in closed vessels, and N_2 bubbling was performed prior to any As^{III} experiments in order to maintain non-oxic conditions. The absence of oxidation was further checked through As^{III} specific measurements. For experiments involving As^{V}, total As (As_T) concentration in the diffusate and retentate were analysed by GFAAS. For experiments involving As^{III}, As concentration in the diffusate and retentate were analysed by GFAAS (As_T) and voltammetry (As^{III}). UV–vis fluorescence measurements were performed on the retentate (both for As^{V} and As^{III}, and for all the experiments), to follow SRHA modifications according to the presence of increasing As concentration (therefore a study of fluorescence quenching), as well as follow the influence of the added cations.

First, the effect of pH on As binding on SRHA was studied. Arsenic concentration (both for As^{III} and As^{V}) was set up around 1.2 μM, corresponding to the middle of the range used for the further studies. By buffering both the retentate and the diffusate [59], various pH values were imposed with organic buffers: 2, 4, 6, 8 and 10.

Then, isotherms were performed by placing increasing As concentrations (from 0.166 to 3.5 μM; either As^{III} or As^{V}) in separated dialysis bag. The pH was buffered at 8.0 ± 0.2 for all these experiments (both the retentate and the diffusate). This value was chosen according to the results of the previous experiments on pH.

Finally, to check the possible role of cations on As binding (either As^{III} or As^{V}), isotherms were repeated but with the addition of 1 mM Na or 1 mM Ca, both in the retentate and the diffusate. The pH was buffered at 8 for all these experiments (both the retentate and the diffusate).

Previously to these experiments involving SRHA and As, a whole series of blank tests were carried out at the same pH and ionic strength conditions: reactors were filled only with mQ water to check possible As or carbon inputs of the vessels. Dialysis membrane carbon inputs were also tested. Arsenic diffusion through the dialysis membrane was also checked in order to assess the absence of any binding by the membrane, which would further account for interactions with SRHA. SRHA diffusion through the membrane was also quantified to check that the membrane cut off was appropriate to contain SRHA and let only free As crossing the membrane. Finally, major ions SRHA content was checked by ionic chromatography.

2.4. Data analysis

2.4.1. Fluorescence quenching mechanism

The nature of the fluorescence quenching was investigated for As–SRHA interaction using the Stern–Volmer equation [58,60]

$$\frac{F_o}{F} = 1 + K_{SV}[As]$$

where: F_o and F are the relative fluorescence intensities of SRHA in absence and in presence of As, respectively; K_{SV} is the Stern–Volmer constant (M^{-1}).

In the case of a linear relationship between F_o/F and As concentration, fluorescence quenching can be considered as purely dynamic or purely static. Oppositely, a non-linear relationship can suggest a combination of dynamic and static quenching mechanisms and/or the presence of at least 2 binding sites [58,60].

2.4.2. Calculation of the SRHA–As binding parameters from isotherm experiments: Model 1

The binding between As (either As^{III} or As^{V}) and SRHA was described by the following reaction:

$$SRHA + As^{III\ or\ V} \Leftrightarrow SRHA - As^{III\ or\ V}$$

The corresponding conditional constants were calculated using the following equations:

$$K^{cond,\,i}_{SRHA-As^{III\ or\ V}} = \frac{[SRHA-\text{bound As}]^i}{[SRHA]^i[\text{free As}]^i} = \times\frac{[SRHA-\text{bound As}]^i}{\left[SRHA_T - [SRHA-\text{bound As}]^i\right][\text{free As}]^i}$$

and $\overline{K}^{cond}_{SRHA-As^{III\ or\ V}} = \frac{\sum_{i=1}^{n} K^{cond,\,i}_{SRHA-As^{III\ or\ V}}}{n}$

where $K^{cond,\,i}_{SRHA-As^{III\ or\ V}}$ is the conditional SRHA–As binding constant calculated from the ith experiment; $\overline{K}^{cond}_{SRHA-As^{III\ or\ V}}$ is the average of the conditional constants calculated from the n experiments; $[SRHA]^i$ and $[SRHA\text{–bound As}]^i$ are the concentrations of "unbound SRHA" and As bound to SRHA, respectively; $[SRHA]_T$ corresponds to the sum of carboxylic and phenolic sites of SRHA (i.e. 13.83 meq g_C^{-1}, [23]); [free As] is the As concentration measured in the diffusate.

2.4.3. Modelling of the effect of Na and Ca onto SRHA–As binding using PHREEQC: Model 2

The SRHA–As interaction parameters (binding constants and site density) were implemented in the PHREEQC database (version 2.11, [61]) in order to simultaneously model all the binding isotherms.

So, Model 2 was defined in order to simulate SRHA–As interaction in the experimental conditions using the solution chemical composition, the protonation reaction of SRHA ($pK_a = 4.42$, Table 1, [23]) and a direct interaction between SRHA and As (either As^{III} or As^{V}) characterised by the calculated ($\overline{K}^{cond}_{SRHA-As^{III\ or\ V}}$) values (Model 1). However, these conditional binding constants were converted to thermodynamic ones in order to correct the "free As" and "unbound SRHA" concentrations from their inorganic side reaction coefficients (α_i) according to the following equations:

$$[H_3AsO_3] = \frac{\left[\text{free } As^{III}\right]}{\alpha_{As^{III}}}$$

$$\left[HAsO_4^{2-}\right] = \frac{\left[\text{free } As^{V}\right]}{\alpha_{As^{V}}}$$

$$[SHRA\_O^-] = \frac{[\text{unbound SRHA}]}{\alpha_{SRHA}}$$

where α_i is the inorganic side reaction coefficient of the species i [62]; $[H_3AsO_3]$, $[HAsO_4^{2-}]$ and $[SRHA\_O^-]$ are the free concentrations of the main form of As^{III}, As^{V} and SRHA in the studied conditions, respectively. These ratios, calculated using PHREEQC at the studied pH and chemical composition, were close to 1.0, 1.08 and 1.37 for SRHA, H_3AsO_3 and $HAsO_4^{2-}$, respectively.

Accordingly, SRHA binding to H_3AsO_3 and $HAsO_4^{2-}$ was characterised by the following reactions:

$$SRHA\_O^- + H_3AsO_3 \Leftrightarrow SRHA\_OH_3AsO_3^-$$

$$SRHA\_O^- + HAsO_4^{2-} \Leftrightarrow SRHA\_OHAsO_4^{3-}$$

Table 1
Summary of the optimised binding parameters describing As^{III} and As^{V} interactions with SRHA in presence/absence of major cations: binding site density, binding reactions and their corresponding conditional (Model 1) or thermodynamic (Model 2) stability constants (see the text for details).

		Site density (meq gC^{-1})	Binding reactions $SRHA\_O^- + H^+ = SRHA\_OH$	Log K^{cond}	Log K^{thermo} 4.42[a]
Model 1	As^{III}–SRHA	13.83[a]		5.7 ± 0.2	
	As^{V}–SRHA			5.9 ± 0.3	
Model 2	As^{III}–SRHA	13.83[a]	$SRHA\_O^- + H_3AsO_3 = SRHA\_OH_3AsO_3^-$		5.7 ± 0.2
	As^{V}–SRHA		$SRHA\_O^- + HAsO_4^{2-} = SRHA\_OHAsO_4^{3-}$		6.0 ± 0.3
	As^{V}–SRHA/Ca		$SRHA\_O^- + HAsO_4^{2-} + Ca^{2+} = SRHA\_OCaHAsO_4^-$		10.03 ± 0.2
			$SRHA\_O^- + HAsO_4^{2-} = SRHA\_OHAsO_4^{3-}$		6.0 ± 0.3
	As^{V}–SRHA/Na		$SRHA\_O^- + Na^+ = SRHA\_ONa$		4.0 ± 0.1
			$SRHA\_O^- + HAsO_4^{2-} = SRHA\_OHAsO_4^{3-}$		6.0 ± 0.3

[a] [30].

Their corresponding thermodynamic constants ($K^{thermo}_{SRHA-As^{III\ or\ V}}$) were calculated as follow:

$$K^{thermo}_{SRHA-As^{III\ or\ V}} = \overline{K}^{cond}_{SRHA-As^{III\ or\ V}} \times \alpha_{SRHA} \times \alpha_{As^{III\ or\ V}}$$

The competition effect of Na on As^{V} binding with SRHA was described by the following reaction and binding constant:

$$SRHA\_O^- + Na^+ \Leftrightarrow SRHA\_ONa$$

and $K_{SRHA-Na} = \frac{[SRHA\_ONa]}{[SRHA\_O^-][Na^+]}$

The ternary interaction between Ca, As^{V} and SRHA was described by the following reaction and binding constant:

$$SRHA\_O^- + Ca^{2+} + HAsO_4^{2-} \Leftrightarrow SRHA\_OCaHAsO_4^-$$

and

$$K_{SRHA-Ca-As^{V}} = \frac{[SRHA\_OCaHAsO_4^-]}{[SRHA\_O^-]\left[Ca^{2+}\right]\left[HAsO_4^{2-}\right]}$$

The values of these 2 binding constants were optimised in order to obtain the minimal value of the goodness-of-fit (ν) between measured and PHREEQC simulated data according to the following equation:

$$\nu = \frac{\sum_{i=1}^{n}\left|\log\left([As]^i_{meas}\right) - \log\left([As]^i_{sim}\right)\right|}{n}$$

where: $[As]^i_{meas}$ and $[As]^i_{sim}$ are the measured and simulated concentrations of As for the ith experiment, respectively.

3. Results and discussion

The initial As content in SRHA (< 13 nM) appeared negligible compared to the As added during the presented experiments and consequently not taken into account hereafter. Furthermore, the major ions measurements revealed the very low amount of major anions and cations in the SRHA solution (below 0.1 mM level) which therefore cannot hinder the experiments performed in this study.

Blank test showed no As or carbon inputs by the used reactors or the dialysis membrane. Furthermore, no As binding on the membrane could be measured (0.42% As lost on average). Concerning membrane cut-off, negligible organic carbon content and no fluorescence were measured in the diffusate, therefore, it can be assumed that no SRHA crossed the dialysis membrane.

3.1. As^{III} and As^{V} binding as a function of pH

Whatever the considered pH, SRHA showed important As^{III} and As^{V} binding (between 30 and 80%; Fig. 1). Binding appeared stronger at neutral to basic pH. At these pH, As^{III} and As^{V} main species are respectively $H_3AsO_3/H_2AsO_3^-$ (pKa=9.29) and $H_2AsO_4^-/HAsO_4^{2-}$/ (pKa=6.96) [63]. For As^{III}, the binding did not fluctuate much, increasing from ~65% at pH 2 to reach a maximum of 75% at pH 8 (Fig. 1). This behaviour was already observed for As^{III}- and Sb^{III}-Aldrich Humic Acid interaction and explained by H^+ and OH^- competition [9,64].

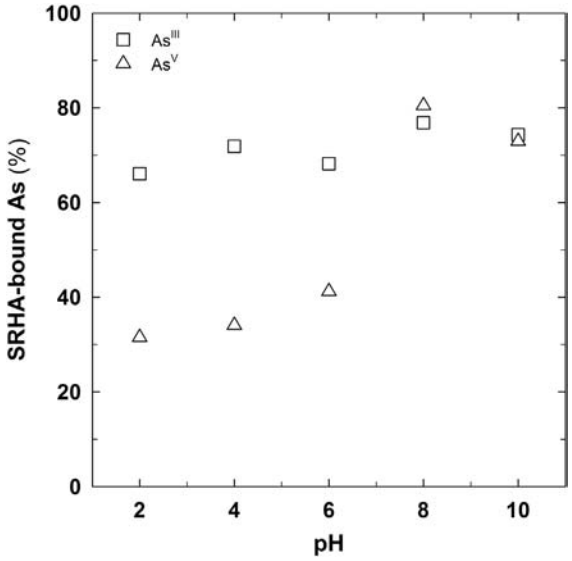

Fig. 1. pH influence on As^{V} (triangle) and As^{III} (square) binding with SRHA. Total arsenic concentration (for both As^{III} and As^{V}) was adjusted to 1.2 μM (see the text for details). The analytical variance falls within the symbol size.

For As^{V}, the retention appeared strongly reduced at acidic pH. The modification of speciation from $H_2AsO_4^-$ to $HAsO_4^{2-}$ corresponds to an important enhancement of the binding from 40 to 80% around pH ~7, a variation not observed for As^{III} whose speciation ranged from neutral to negative species by increasing the pH. The weaker binding of As^{V} at acidic pH is in agreement with results from the literature [9,10]. However, this finding went oppositely to what was expected from theoretical considerations. As a matter of fact, at acidic pH, As and SRHA global charge were neutral [23,65]. On the contrary, at neutral to basic pH, As and SRHA global charge were negative [23]. As proposed by Buschmann et al. [9], a possible explanation could be the high formal charge of As^{V} centre reacting with phenolate group of SRHA.

According to the binding results, all the following experiments were performed at pH 8.0 ± 0.2, by buffering the retentate and the diffusate, which implies that the main species were H_3AsO_3 and $HAsO_4^{2-}$ for As^{III} and As^{V}, respectively.

3.2. As–SRHA binding isotherms and fluorescence quenching

3.2.1. As^{III} binding to SRHA

The relationship between SRHA–bound As and total As^{III} concentrations during the isotherm experiment was quasi-linear (Fig. 2A), with an overall slope of 0.38 ($r^2=0.99$), apparently showing no saturation of SRHA binding sites in the studied conditions. The addition of monovalent (Na) or divalent (Ca) cations had no effect on As^{III} binding by SRHA. Either phenolates or carboxylates functions may constitute the specific binding site to neutral As^{III} species leading to a direct interaction between As^{III} and SRHA. Such results were already observed for Aldrich Humic Acid toward As^{III} and As^{V} [9].

Concerning UV–visible fluorescence, each EEM spectrum was successfully reconstructed by a linear combination of 2 components (hereafter named C1 and C2) with 98.5% of recovery. These two components were characteristic of humic acids and proteins, respectively (peak A and M, and peak T according to [50], Fig. SI-1). As similar trends were observed for the two components (Fig. SI-2), only the results on C1 are discussed hereafter.

A fluorescence quenching phenomena was clearly observed during As^{III} additions (Fig. 3A). As already observed during the isotherm experiment, the presence of Na or Ca seemed not to affect As^{III}–SRHA binding, neither on SRHA–bound As quantity nor on SRHA fluorescence quenching (Figs. 2A and 3A). The observed linear trend in Stern–Volmer plot ($r^2=0.87$, Fig. 3A) indicated a single quenching mechanism, either dynamic or static. In 3 conditions (i.e. As^{III} alone, with Na or Ca), the Stern–Volmer constants were similar and close to $\sim 0.16\ M^{-1}$. These results confirmed that a direct binding on a single fluorophore group was responsible of the As^{III}–SRHA interaction. Such SRHA binding sites appeared to be specific to As^{III} and not influenced by the presence of major cations.

3.2.2. As^{V} binding to SRHA

The SRHA–bound As concentration rose with increasing total As^{V} concentration but with an amplitude depending on the solution composition (Fig. 2B). In absence of cations, the relationship was quasi-linear for As^{V} binding with an overall slope of 0.46 ($r^2=0.98$). The close slopes observed for As^{III} and As^{V} binding without cation addition could indicate a common mechanism, as already suggested by the close percentage of SRHA–bound As^{III} and As^{V} at pH 8 (Fig. 1). As^{V} binding in presence of 1 mM Ca was also quasi-linear but with a higher slope of 0.78 ($r^2=0.99$). This enhanced binding can be explained by a different mechanism, probably implying a cationic bridge. As^{V} binding in presence of Na rapidly reached a stable value independent of the total added As concentration (Fig. 2B). An explanation could be the competition of Na on the same SRHA binding sites, therefore reducing As^{V} binding capacity.

When comparing the Stern–Volmer plots of As^{V} and As^{III} (Fig. 3B–D), the presence of cations also clearly influenced the fluorescence quenching mechanism. Indeed, with As^{V} alone, the Stern–Volmer plot appeared to be non-linear (Fig. 3B). Such trend probably indicates a mixed static/dynamic quenching mechanism or an heterogeneity of the SRHA binding sites toward As^{V} [60]. Oppositely, in presence of Na, the Stern–Volmer plot returned to linearity with values similar to that observed for As^{III} (Fig. 3C). So, the addition of Na induced a change in SRHA binding, probably due to Na competition on SRHA binding sites. The As^{V} binding capacity was then apparently reduced to the group of sites responsible for As^{III} binding. In presence of Ca, the observed enhanced binding of As^{V} by SRHA (Fig. 2B) resulted in an absence of noticeable variation of the corresponding Stern–Volmer plot (Fig. 4D) with a Stern–Volmer constant of ~ 0.01. Such variation clearly suggests that Ca acted as a cationic bridge on the binding of As^{V} by SRHA, which induced cancelling the As^{V} quenching effect.

3.3. Modelling of As–SRHA binding, implication in arsenic speciation determination

The previous results have suggested: (i) a similar direct interaction for As^{III} and As^{V} binding on SRHA, (ii) a cationic bridge mechanism when considering As^{V} binding in presence of Ca, and (iii) a competition for SRHA binding sites between As^{V} and Na. In order to demonstrate that such mechanisms were occurring and to propose a set of binding parameters usable in any speciation code, the modelling of the obtained data was performed.

The calculated conditional As–SRHA interaction constants (Section 2.4.2) were of 5.7 ± 0.2 and 5.9 ± 0.3 for As^{III} and As^{V} respectively (Model 1, K^{cond}, Table 1). The same approach was applied on the As–SRHA isotherm data published by Buschmann et al. [9], resulting in similar values ($\log K^{cond}$ of 5.2 ± 0.4 and 5.6 ± 0.5 for As^{III} and As^{V} respectively) which validates the applied approach.

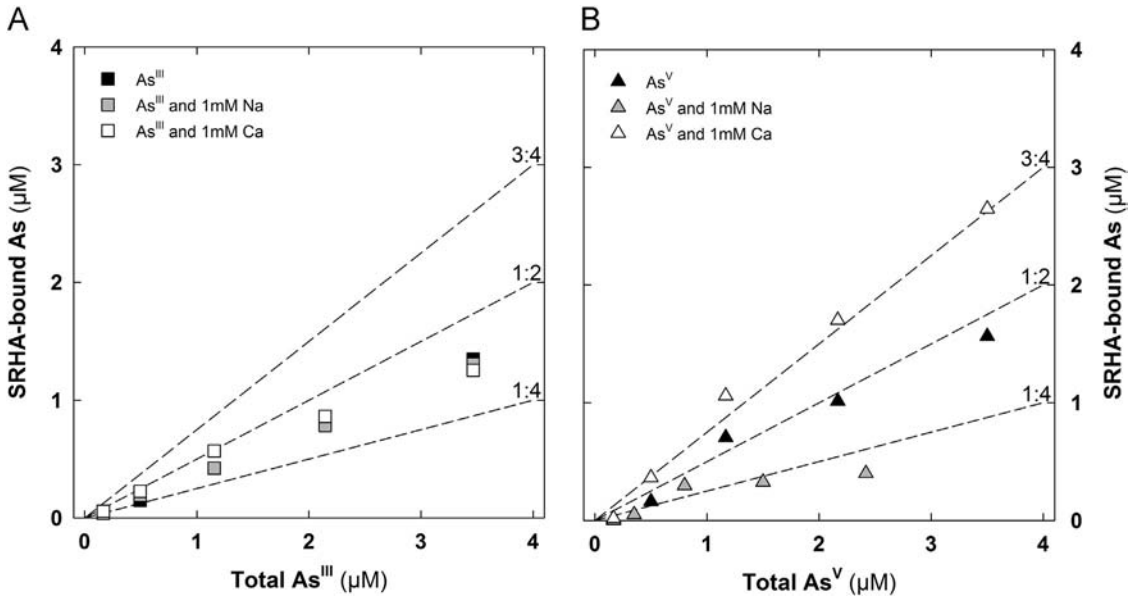

Fig. 2. SRHA–bound As^{III} (A) and As^{V} (B) as a function of total As concentration, in absence (closed symbols) or in presence of Na and Ca (grey and open symbols, respectively). The experimental pH was adjusted to 8.0 ± 0.2. The analytical variance falls within the symbol size.

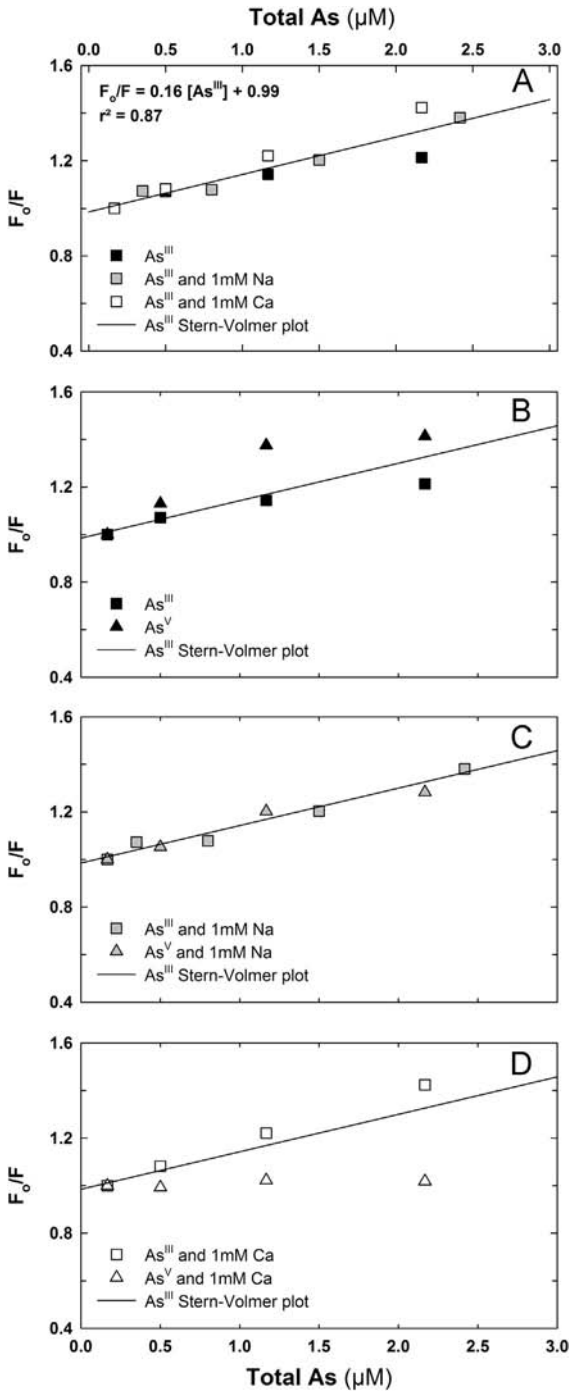

Fig. 3. Stern–Volmer representation of the quenching of SRHA C1 fluorophore by (A) As^{III} in absence/presence of Na and Ca, (B) As^{V} alone, As^{V} in presence of (C) Na and (D) Ca.

Scatchard linearization [66] was performed on isotherms data with As^{III} and As^{V} alone (data not shown) in order to calculate the corresponding SRHA binding site. The obtained values were of 14.6 ± 1.5 and 16.4 ± 1.5 meq gC^{-1} for As^{III} and As^{V}, respectively. Such values appeared to be very close to the sum of carboxylic and phenolic sites (13.83 meq gC^{-1}) obtained by acid-base titration modelling, justifying the use of this value as SRHA binding site for As. Scatchard linearization of As^{V} isotherms in presence of Na and Ca led to SRHA binding site of 3.1 ± 0.9 and 21.3 ± 6.1 meq gC^{-1}, as depicted on Fig. SI-3. These results respectively confirmed an attenuation and enhancement of the SRHA affinity for As^{V}.

Accordingly, a unified modelling approach (Model 2) was proposed in order to depict all these variations with a unique set of binding parameters (Table 1): (i) the conditional binding constants from Model 1 converted into thermodynamic ones (see Section 2.4.3), (ii) the SRHA total binding sites density ($SRHA_T = 13.83$ meq gC^{-1}) and its corresponding acidity constant (pKa = 4.42) [23], (iii) the Na and Ca effects onto As^{V} binding described by their binding constants. All these parameters were implemented in the PHREEQC speciation database in order to simulate As^{III} and As^{V} dialysis experiments.

The corresponding fitting line satisfactory reproduced the measured data (Fig. 4A and B), validating the proposed model and the hypothesis of a direct binding of SRHA with H_3AsO_3 and $HAsO_4^{2-}$. As shown on Fig. 4C, the competition effect of Na onto As^{V} binding by SRHA can be fitted as well adding in Model 2 a binding constant ($\log K = 4.0 \pm 0.1$) for the SRHA_ONa species, which induced a decrease of the available SRHA sites for As^{V}. Additionally, the enhanced SRHA–bound As^{V} in presence of Ca (Fig. 4D) was correctly fitted including a binding constant ($\log K = 10.3 \pm 0.2$) for the $SRHA\_OCaHAsO_4^-$ ternary complex, in competition with the $SRHA\_OHAsO_4^{3-}$ one. However, the saturation of SRHA binding sites at high As^{V} concentration induced a divergence between the measured points and the fitting line, the former being above (Fig. 4D). If not resulting from analytical uncertainty, such deviation could suggest that Ca addition not only enhanced the SRHA–As^{V} binding strength but also the binding sites density by generating new binding sites onto the SRHA unavailable in absence of Ca, as intimated by Scatchard linearization. Further studies will be required to validate or not this observation.

4. Environmental considerations

The analytical and modelling tools used in this study allowed proving that the mechanism of As^{III} and As^{V} binding on SRHA depends on the As species and the co-occurring cations. Concerning As^{III}, in the considered cases, whatever the pH and the cation in presence (monovalent or divalent), the mechanism of binding did not vary. This was confirmed by the experimental results, the modelling and the fluorescence measurements. Concerning As^{V}, in the considered cases, the presence of a monovalent cation did not modify the binding mechanism but decreased the binding sites and therefore the binding capacity. Contrarily, As^{V} binding was significantly enhanced by the addition of a divalent cation, and the formation of a ternary complex SRHA–Ca–As was evidenced both by modelling and the fluorescence results. To our knowledge, this evidence has never been presented before. Additionally, the magnitude of such bonds suggested that this kind of complexation could play a role in regulating As mobility and bioavailability in ecosystems. For instance, our previous work on As and Fe colloids in anoxic groundwaters and soil interstitial waters from paddy fields in Bangladesh [67] demonstrated independent speciation of Fe and As. As a matter of fact, in such anoxic conditions, Fe was mainly found as colloids whereas As was mainly encountered as oxyanion, As distribution was therefore proven independent of Fe. In this case, organic matter could so be the leading parameter governing As distribution through specific complexation sites, as also suggested for instance in deep/anoxic porewaters from coastal sediments [4].

Furthermore, this works provides the environmentalist community with new binding parameters describing the affinity of organic matter as humate (a usual dissolved organic matter in speciation code) to As^{III} and As^{V}, which could be implemented in speciation databases for future studies dedicated to As distribution in environments rich in organic matter.

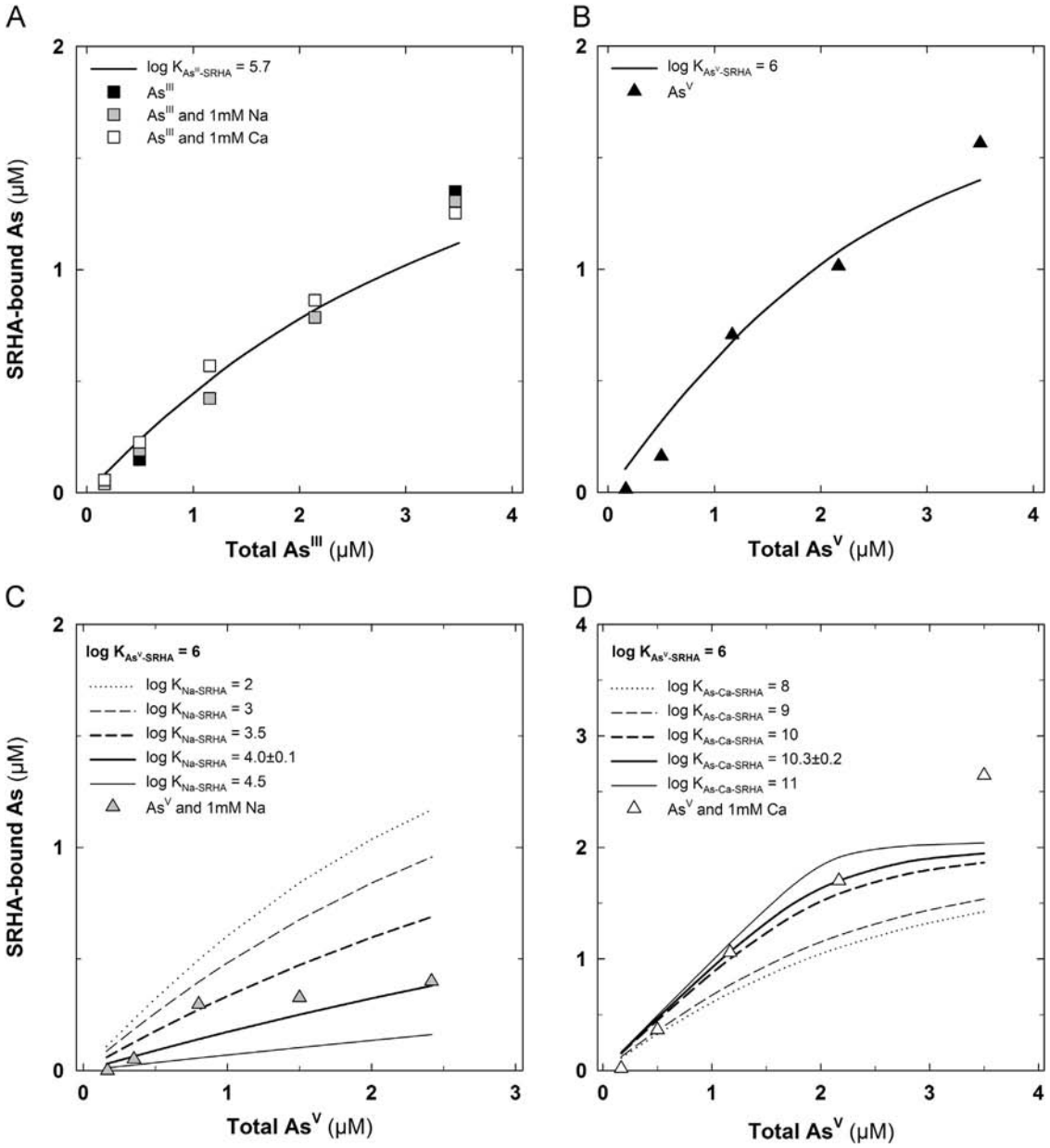

Fig. 4. SRHA–bound As as a function of the total concentration of (A) As^{III} in absence/presence of Na and Ca, (B) As^{V} alone, As^{V} in presence of (C) Na and (D) Ca. On each graph, the thick line represents PHREEQC fitting using the optimised binding parameters from Model 2 (see Table 1). The other lines depicted on graphs (C) and (D) show the PHREEQC fitting obtained when varying Na–SRHA and As^{V}–Ca–SRHA binding stability constants, respectively (see the text for details).

Appendix A. Supporting information

Supplementary data associated with this article can be found in the online version at http://dx.doi.org/10.1016/j.talanta.2014.11.053.

References

[1] A.J. Bednar, J.R. Garbarino, M.R. Burkhardt, J.F. Ranville, T.R. Wildeman, Water Res. 38 (2004) 355–364.
[2] M. Ponthieu, P. Pinel-Raffaitin, I. Le Hecho, L. Mazeas, D. Amouroux, O.F. X. Donard, et al., Water Res. 41 (2007) 3177–3185.
[3] M.L. Kile, E. Hoffman, Y.-M. Hsueh, S. Afroz, Q. Quamruzzaman, M. Rahman, et al., Environ. Health Perspect. 117 (2009) 455–460.
[4] D.H. Dang, E. Tessier, V. Lenoble, G. Durrieu, D. Omanović, J.-U. Mullot, et al., Mar. Chem. 161 (2014) 34–46.
[5] K. Farzana Akter, Z. Chen, L. Smith, D. Davey, R. Naidu, Talanta 68 (2005) 406–415.
[6] R. Zhao, M. Zhao, H. Wang, Y. Taneike, X. Zhang, Sci. Total Environ. 371 (2006) 293–303.
[7] R.E. Rivas, I. López-García, M. Hernández-Córdoba, Acta Part B At. Spectrosc. 64 (2009) 329–333.
[8] L.B. Escudero, E.M. Martinis, R.A. Olsina, R.G. Wuilloud, Food Chem. 138 (2013) 484–490.
[9] J. Buschmann, A. Kappeler, U. Lindauer, D. Kistler, M. Berg, L. Sigg, Environ. Sci. Technol. 40 (2006) 6015–6020.
[10] G. Liu, A. Fernandez, Y. Cai, Environ. Sci. Technol. 45 (2011) 3210–3216.
[11] M. Erk, B. Raspor, J. Electroanal. Chem. 502 (2001) 174–179.
[12] M.T.S.D. Vasconcelos, M.F.C. Leal, Mar. Chem. 75 (2001) 123–139.
[13] J. Buffle, Natural organic matter and metal–organic interactions in aquatic systems, in: H. Sigel, (Eds.), Metal Ions in Biological Systems, M. Dekker, New York, 1984.
[14] R. Liu, J.R. Lead, A. Baker, Chemosphere 68 (2007) 1304–1311.
[15] B. Seredyńska-Sobecka, A. Baker, J.R. Lead, Water Res. 41 (2007) 3069–3076.
[16] N. Ates, M. Kitis, U. Yetis, Water Res. 41 (2007) 4139–4148.
[17] A. Baker, E. Tipping, S.A. Thacker, D. Gondar, Chemosphere 73 (2008) 1765–1772.
[18] M. Bieroza, A. Baker, J. Bridgeman, Sci. Total Environ. 407 (2009) 1765–1774.
[19] S. Mounier, R. Braucher, J.Y. Benaim, Water Res. 33 (1999) 2363–2373.
[20] N. Her, G. Amy, J. Chung, J. Yoon, Y. Yoon, Chemosphere 70 (2008) 495–502.
[21] U. Lankes, H.-D. Lüdemann, F.H. Frimmel, Water Res. 42 (2008) 1051–1060.
[22] Y. Lu, H.E. Allen, Water Res. 36 (2002) 5083–5101.
[23] J.D. Ritchie, E.M. Perdue, Geochim. Cosmochim. Acta 67 (2003) 85–96.
[24] S. Mounier, H. Zhao, C. Garnier, R. Redon, Biogeochemistry 106 (2011) 107–116.
[25] W.B. Chen, D.S. Smith, C. Guéguen, Chemosphere 92 (2013) 351–359.

[26] D.K. Ryan, J.H. Weber, Anal. Chem. 54 (1982) 986–990.
[27] X. Wang, Y. Lv, X. Hou, Talanta 84 (2011) 382–386.
[28] J. Matschullat, Sci. Total Environ. 249 (2000) 297–312.
[29] B. Mandal, K. Suzuki, Talanta 58 (2002) 201–235.
[30] J.A. Wilkie, J.G. Hering, Colloids Surf. A: Physicochem. Eng. Asp. 107 (1996) 97–110.
[31] E. Lombi, W.W. Wenzel, R.S. Sletten, J. Plant Nutr. Soil Sci. 162 (1999) 451–456.
[32] M.P. Elizalde-González, J. Mattusch, R. Wennrich, J. Environ. Monit. 3 (2001) 22–26.
[33] V. Lenoble, O. Bouras, V. Deluchat, B. Serpaud, J. Bollinger, J. Colloid Interface Sci. 255 (2002) 52–58.
[34] G.C. Saha, M.A. Ali, Sci. Total Environ. 379 (2007) 180–189.
[35] R.-M. Couture, C. Gobeil, A. Tessier, Geochim. Cosmochim. Acta 74 (2010) 1238–1255.
[36] J.-M. Garnier, F. Travassac, V. Lenoble, J. Rose, Y. Zheng, M.S. Hossain, et al., Sci. Total Environ. 408 (2010) 4185–4193.
[37] K. Kalbitz, R. Wennrich, Sci. Total Environ. 209 (1998) 27–39.
[38] M. Bauer, C. Blodau, Sci. Total Environ. 354 (2006) 179–190.
[39] P. Sharma, A. Kappler, J. Contam. Hydrol. 126 (2011) 216–225.
[40] M. Grafe, M.J. Eick, P.R. Grossl, A.M. Saunders, J. Environ. Qual. 31 (2002) 1115–1123.
[41] H.-T. Lin, M.C. Wang, G.-C. Li, Chemosphere 56 (2004) 1105–1112.
[42] P. Warwick, E. Inam, N. Evans, Environ. Chem. 2 (2005) 119.
[43] K. Ritter, G.R. Aiken, J.F. Ranville, M. Bauer, D.L. Macalady, Environ. Sci. Technol. 40 (2006) 5380–5387.
[44] G. Liu, Y. Cai, Chemosphere 81 (2010) 890–896.
[45] P. Sharma, J. Ofner, A. Kappler, Environ. Sci. Technol. 44 (2010) 4479–4485.
[46] Y. Louis, C. Garnier, V. Lenoble, D. Omanović, S. Mounier, I. Pizeta, Mar. Environ. Res. 67 (2009) 100–107.
[47] V. Lenoble, C. Chabroullet, Ral Shukry, B. Serpaud, V. Deluchat, J. Bollinger, J. Colloid Interface Sci. 280 (2004) 62–67.
[48] V. Lenoble, C. Garnier, a. Masion, F. Ziarelli, J.M. Garnier, Anal. Bioanal. Chem. 390 (2008) 749–757.
[49] Y. He, Y. Zheng, M. Ramnaraine, D.C. Locke, Anal. Chim. Acta 511 (2004) 55–61.
[50] P.G. Coble, Mar. Chem. 51 (1996) 325–346.
[51] C.M. Neculita, Y. Dudal, G.J. Zagury, J. Environ. Sci. 23 (2011) 891–896.
[52] C.A. Stedmon, S. Markager, R. Bro, Mar. Chem. 82 (2003) 239–254.
[53] X. Luciani, S. Mounier, H.H.M. Paraquetti, R. Redon, Y. Lucas, A. Bois, et al., Mar. Environ. Res. 65 (2008) 148–157.
[54] X. Luciani, S. Mounier, R. Redon, A. Bois, Chemom. Intell. Lab. Syst. 96 (2009) 227–238.
[55] D.H. Dang, V. Lenoble, G. Durrieu, J.-U. Mullot, S. Mounier, C. Garnier, Estuar. Coast. Shelf Sci. 151 (2014) 100–111.
[56] S.E. Cabaniss, Environ. Sci. Technol. 26 (1992) 1133–1139.
[57] A. Manciulea, A. Baker, J.R. Lead, Chemosphere 76 (2009) 1023–1027.
[58] J. Michon, S. Frelon, C. Garnier, F. Coppin, J. Fluoresc. 20 (2010) 581–590.
[59] R.C. Weast, Handbook of Chemistry and Physics, The Chemical Rubber Co., Ohio, USA, 1972.
[60] J.R. Lackowicz, Principles of Fluorescence Spectroscopy, 3rd ed., Springer, 2006.
[61] D. Parkhurst, C.A.J. Appelo, U.S. Geol. Surv. Water-Resourc. Investig. Rep. (1999) 99–4259.
[62] Y. Louis, C. Garnier, V. Lenoble, S. Mounier, N. Cukrov, D. Omanović, et al., Mar. Chem. 114 (2009) 110–119.
[63] A.E. Martell, R.M. Smith, R.J. Motekaitis, NIST Critical Stability Constants of Metal Complexes Database, 2002.
[64] J. Buschmann, L. Sigg, Environ. Sci. Technol. 38 (2004) 4535–4541.
[65] C. Garnier, S. Mounier, J.Y. Benaim, Water Res. 38 (2004) 3685–3692.
[66] G. Scatchard, Ann. N. Y. Acad. Sci. 51 (1949) 660–672.
[67] J.-M. Garnier, C. Hurel, V. Lenoble, C. Garnier, K.M. Ahmed, J. Rose, Geochemistry 26 (2011) 1665–1672.